Simulation of the laser beam welding process by applying a double-ellipsoid heat flux distribution

Anders F. Mikkelstrup, Craig M. Farley, Kristoffer Stampe,
Marc M. Kristensen & Mathias E. Thomsen

Department of Materials and Production, Aalborg University
Fibigerstraede 16, DK-9220 Aalborg East, Denmark
Email: vt2gr4105b@m-tech.aau.dk,
Web page: http://www.mechman.m-tech.aau.dk/

Abstract
A coupled thermal-mechanical analysis is used to model the process of joining a T-piece by deep penetration laser beam welding. As the aim is to provide information about the welding induced stress, the distortion and temperature distribution of the welded component, a conduction heat transfer based model is used. The moving heat source is modelled based on Goldak's double-ellipsoid heat flux distribution, requiring a-priori knowledge about the dimensions of the weld pool or the Goldak parameters. Initially, the Goldak parameters are determined by experimentally measuring the keyhole of a laser beam weld performed with a pre-determined reference power input. By comparing the surface heat distribution of the model with experimental data, the efficiency of the power input from the laser beam is determined. The efficiency is used to adjust the power input in the model, so that the resulting surface heat distribution is similar to the experimental data. To ensure the robustness of the model, the model's performance is furthermore evaluated at power inputs $\pm 10\%$ of the pre-determined reference power input. As the size of the weld pool varies with the power input, the Goldak parameters are analytically estimated for power inputs different from the pre-determined and experimentally validated reference by assuming a constant penetration depth. The results show that it is possible to replicate the temperature distribution at specific points with a deviation below 10%. Furthermore, assuming that the size of the weld pool does not change with the an increase or decrease of 10% of the power inputs, is concluded to be a valid assumptions. Analytically determining the size of the weld pool, while assuming a constant penetration depth, yielded the same deviation as assuming a constant size of the weld pool.

Keywords: Coupled FEA, LS-DYNA, laser beam welding, heat source model, temperature distribution, experimental calibration

1. General Introduction

Laser beam welding (LBW) is characterised by its high power density, which is achieved by focussing electromagnetic radiation into a fine spot; thus enabling the ability to create deep and narrow penetration welds. High speeds, a small heat affected zone and lower distortion and residual stresses can furthermore be attained as a result of the high energy concentration, which in turn limits the amount of metallurgical damage and distortion [1][2].

These advantages underline why the adoption of LBW as a process for part assembly is becoming increasingly popular in industrial manufacturing. A consequence of this is that it poses new challenges with respect to process knowledge and expertise. An example of this is Grundfos A/S, who are currently experiencing problems in connection with the LBW process of their impeller blades, as the target welding trajectory deviates from the actual trajectory due to welding induced distortion. This complicates the subsequent production steps and negatively influences the efficiency of the pumps.

Fig. 1 illustrates the impeller and the deviation of the welding trajectory.

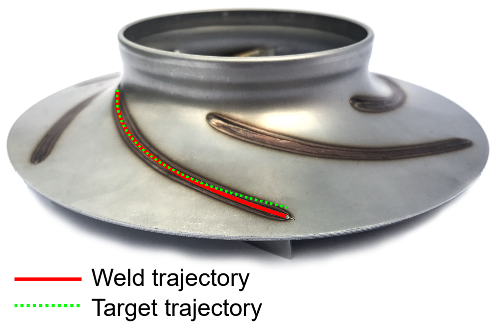

Fig. 1 Illustration of the T-joint laser welding, where the weld trajectory diverges from the target trajectory. The target trajectory is determined by the position of the impeller blade.

Modelling the LBW process can be a highly efficient tool for research and production engineering, as it enables the ability to obtain detailed information in regards to the characteristics of the weld pool and the welding parameters, i.e. welding speed, beam diameter, heat input, etc. [3]. Using LS-DYNA, the LBW process can be simulated by performing a non-linear coupled thermal-mechanical analysis with the purpose of replicating, and possibly predicting both the temperature distribution and the welding induced distortion of the Grundfos impeller. Due to the complex geometry of the impeller, the model is however based on a melt-through T-joint consisting of two sheet metal plates, as this is considered to be a simple, representative model.

When modelling the LBW process, caution must be exercised, as [4] states, LBW involves a series of complex phenomena; ionization and vaporization of material, the formation of a keyhole, solidification at the liquid-solid interface and stirring of the weld poll due to buoyancy, etc. Hence, underlining the importance of experimental validation of the model.

[5] states that the most critical issue in the thermal analysis of LBW is correctly modelling the weld pool and corresponding heat input in the material. The fact that the vertex angle of the nearly conically shaped keyhole decreases as the depth increases, contributes to the challenge of obtaining a realistic definition of the heat source [5] [6]. The simple and computationally inexpensive conduction heat transfer based models are widely used in coupled thermal-mechanical analysis, especially when the temperature distribution over a large domain is essential [7]. One must be aware, that the reliability of such models is highly sensitive to how the heat source is modelled [8].

Several researchers have proposed methods on how to simulate the size and shape of the weld pool with the linear heat conduction model by [9], being the simplest [3]. [10] was the first to suggest a distributed heat source, the "disc model", which is based on a circularly Gaussian distributed heat flux and centred at the origin in the z-z plane. The disc model deposits the heat directly at the surface and is therefore not well suited for deep penetration welds, e.g. welds created by high density welding methods, such as laser welding or electron beam welding. [11] further developed this concept by introducing the concept of a volumetric heat source via utilizing a double-ellipsoid based on a Gaussian heat flux distribution, suitable for deep penetration welds.

This article aims to model the LBW process by applying the double-ellipsoid heat flux distribution to determine welding-induced distortion.

2. Modelling of Heat Source

The double-ellipsoidal volumetric heat source, proposed by [11], consists of four characteristic length parameters; a, b, c_f and c_r which are illustrated by Fig. 2. These are referred to as the Goldak parameters.

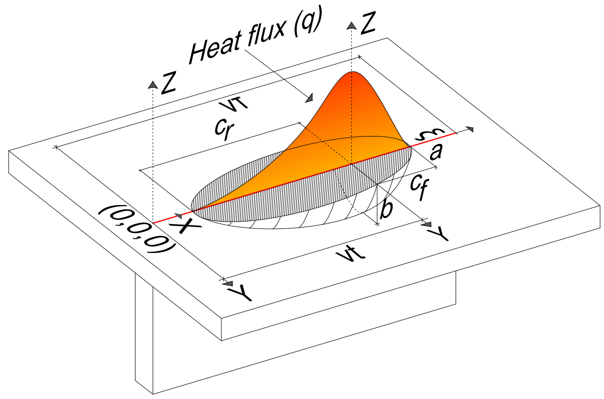

Fig. 2 Illustration of the double ellipsoidal power density distribution including the four characteristic length parameters.

The Gaussian distributed power density is placed at (0,0,0) of the local coordinate system in the shape of a double ellipsoid. This enables the possibility of representing the steep temperature gradient at the front of the heat source and the trailing temperature gradient at the rear, that occurs during laser welding [11]. For weighting the heat distribution in the ellipsoid, the fractions f_f and f_r are used, representing respectively the front and the rear of the ellipsoid; hence the following must apply: $f_f + f_r = 2$. The best correspondence between the measured and calculated thermal history is according to [11] obtained by using $f_f = 0.6$ and $f_r = 1.4$

[11] proposes that the ellipsoid can be described based on conversion of energy and the geometric considerations of the double ellipsoid, yielding the following expression for the power density q, Eq. (1):

$$q(x, y, \xi) = \frac{6\sqrt{3} f_i Q}{abc\pi\sqrt{\pi}} \cdot \exp\left(\frac{-3y^2}{a^2}\right) \exp\left(\frac{-3z^2}{b^2}\right) \exp\left(\frac{-3\xi^2}{c_i^2}\right) \quad (1)$$

Q is the power input, while a, b and c_i[1] are the Goldak parameters. As it is preferable to use a fixed coordinate system, ξ is used to relate the fixed coordinate system of the workpiece, to the local coordinate system of the heat source. This is done by describing the distance between the coordinate systems along the welding direction. This is accomplished by utilizing a lack factor τ, describing the position of the heat source at the beginning of the weld ($t = 0$). If ν is the welding speed, ξ can be expressed by equation (2):

$$\xi = z + \nu(\tau - t) \quad (2)$$

Because of its simplicity and well documented results, the double ellipsoid is chosen as the conduction heat transfer based model, used for modelling the moving heat flow across the surface of the T-joint [7].

2.1 Theory of Goldak Parameter Determination

The necessity of determining the Goldak parameters limits the predictive capability of the model, as these are normally approximated from experimentally measuring the actual weld pool dimensions. In this case, a experimental reference weld is initially used to determine the width of the weld pool and the penetration depth of the key hole. [11] suggests that it is reasonable to take one half of the width of the weld pool to equal the distance in front, and twice the width as being equal to the distance behind the heat source.

[12] proposes that the Goldak parameters for deep penetration welds can be estimated, based on an extended version of a non-dimensional method developed by [13].

[1]The subscript i denotes whether the c defines the front or rear of the ellipsoid, respectively $i = f$ or $i = r$.

The approach uses an operating parameter n, developed for deep penetration welds, given by equation (3):

$$n = \frac{Q}{2\pi kh\left(T_c - T_0\right)} \quad (3)$$

Where k and h are the thermal conductivity and the penetration depth, respectively, while T_0 and T_c define the ambient temperature of the weld and a reference temperature. The latter is usually defined as the melting temperature of the material.

The ellipsoid is here considered in 2D with the Christensen [13] parameters ψ, λ and ρ illustrated in Fig. 3.

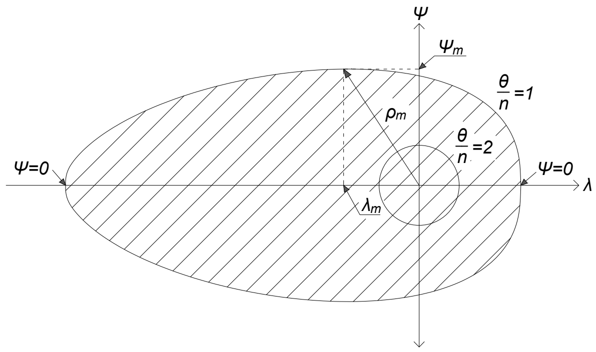

Fig. 3 2D double ellipsoid, illustrating the Christensen parameters.

It follows from [9] that the temperature at any point of a 2D heat flow can be expressed by equation (4).

$$T = T_0 + \frac{Q}{2\pi kh}\left[\exp\left(-\frac{\nu\xi}{2\alpha}\right) K_0\left(\frac{\nu r}{2\alpha}\right)\right] \quad (4)$$

With the use of the Christensen parameters, a modified Bessel function of second order, zero kind K_0, and equation (4), [12] has derived equation (5).

$$\frac{\theta}{n} = \left[\exp\left(-\lambda\right)\right] K_0(\rho) \quad (5)$$

θ is a non-dimensional temperature and expresses the relationship between the temperature at a given point T and T_c with respect to the ambient temperature T_0. As the calculations aim to estimate the size of the fusion zone (FZ), the reference temperature is assumed to be equal to the melting temperature; hence θ is set to 1.

The distance from the origin of the heat source to the point on the axis of the welding direction, where the ellipsoid is widest λ_m, can be estimated by equation (6). This includes making use of a modified Bessel function of second order, first kind K_1.

$$\lambda_m = -\frac{-\rho_m K_0(\rho_m)}{K_1(\rho_m)} \quad (6)$$

Substituting equation (6) into equation (5) by $\lambda = \lambda_m$, yields equation (7), consisting of ρ_m as the only variable.

$$\frac{\theta}{n} = \left[\exp\left(\frac{\rho_m K_0(\rho_m)}{K_1(\rho_m)}\right)\right] K_0 \rho_m \tag{7}$$

Using equation (6) and (7), it is hence possible to compute ρ_m and λ_m. As the ρ_m, λ_m and ψ_m vectors make up respectively the hypotenuse and the catheti of an orthogonal triangle. The values of ρ_m and λ_m can furthermore be used to compute the maximum width of the ellipsoid ψ_m by applying Pythagoras' theorem, equation (8):

$$\psi_m = \sqrt{\rho_m^2 - \lambda_m^2} \tag{8}$$

It must be noted, that ψ_m is equal to the previously mentioned a factor of the Goldak parameters. The c_r and c_f parameters are estimated in relation to the above-mentioned guidelines suggested by [12].

3. Modelling of Heat Dissipation

Modelling of the heat dissipation is furthermore an important aspect in order to ensure a valid and accurate simulation of the laser welding process. This includes a series of physical phenomena, that influence the heat dissipation, i.e convection, radiation and conduction, as in Fig. 4 .

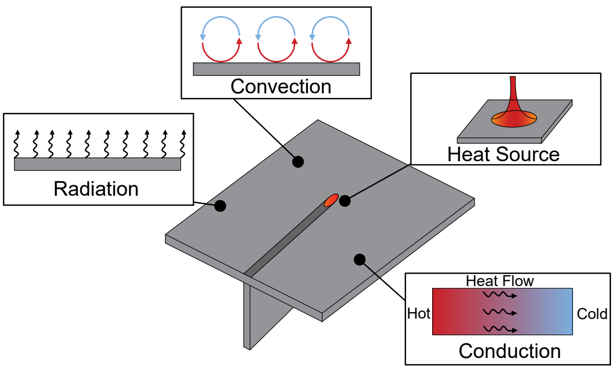

Fig. 4 Illustration of the different topics covered in the modelling of the heat dissipation.

3.1 Convection

In convection, heat is transferred via the movement of molecules caused by temperature differences. In the LBW process, convection occurs when the air-molecules close to the heat source are heated to a higher kinetic energy state than the ambient air-molecules, causing them to drift away. The cooler molecules then move in to replace them, which initiates a circulation of hot and cold air-molecules. This circulation transfers heat from the blank to the ambient surroundings, as illustrated in Fig. 4 [14].

In general, there are two general types of convection, defined as either free or forced. Forced convection refers to convection where the fluid/gas is forced to move relative to the surface. Free convection refers to the case where fluid/gas is not influenced by any external forces e.g. stagnant air. As a result, forced convection has a higher convective heat transfer coefficient than free convection [14].

The governing equation for convection is by eq.(9):

$$q_{conv} = h \cdot (T_{surface} - T_\infty) \tag{9}$$

where q_{conv} is the heat transference that is dissipated to the environment through the surface of the blank by convection, h is the convective heat transfer coefficient and $(T_{surface} - T_\infty)$ is the temperature potential between the object and the ambient environment.

In the experimental set-up, a flow of air is used to keep residue from entering the laser during welding. To incorporate this effect in the model, the convection is modelled as forced. According to [15], the convection coefficient of forced convection with moderate blowing is 0.1 $\frac{mW}{mm^2K}$. The forced convection can be directly implemented in the model via the keyword setting BOUNDARY_CONVECTION.

3.2 Radiation

Radiation is the only type of heat transference, that does not depend on the movement of molecules. Instead, heat is transmitted by electromagnetic waves due to vibrating molecules. The amount of radiation emitted by an object depends on the surface area of the object and on the temperature of the object [16]. The governing equation for radiation is the Stefan Boltzmann equation, given by eq. (10) [16]:

$$P_{rad} = \sigma \cdot A_{surface} \cdot \epsilon \cdot (T_{surface}^4 - T_\infty^4) \tag{10}$$

with P_{rad} being the power radiated from a part with specified surface area $A_{surface}$, while σ and ϵ is respectively the Stefan Boltzmann constant and the emissivity, specifying the fraction of energy emitted from the surface [16].

$$q_{rad} = \sigma \cdot \epsilon \cdot F \cdot (T_{surface}^4 - T_\infty^4) \tag{11}$$

where q_{rad} is the heat flux dissipated to the environment as a result of radiation. F is an exchange factor, which is used to describe where the heat flux is dissipated to. In this case, it is set to 1, specifying that the heat is dissipated from the specimen to the ambient environment [17]. The emissivity factor ϵ of a sheet of rolled stainless steel is set to 0.8 [18].

The LS-DYNA model uses a slightly rewritten equation for radiation by applying the heat flux from the surface. As it is a function of temperature, it is used at every time-step to calculate the dissipated heat flux factor $FMULT$, which states the amount of heat flux that has dissipated to the environment as a result of radiation. $FMULT$ is given by eq. (11).

$$FMULT = \sigma \cdot \epsilon \cdot F = 4.536 \cdot 10^{-11} \frac{mJ}{s \cdot mm^2 \cdot K^4} \tag{12}$$

3.3 Conduction

In conduction, also known as diffusion, heat is transferred by microscopic collisions of particles, such as molecules, atoms and electrons, as well as the movement of electrons within a body [14]. Conduction happens in all matter, such as solids, liquids, gases and plasmas. The principle is illustrated in Fig. 4. The rate at which energy is conducted as heat between two objects is dependent on the temperature difference between the two objects and the material properties such as thermal conductivity, the specific heat capacity and the density of the material. The governing partial differential equation applied for describing three dimensional transient heat conduction in the T-joint is given by eq. (13) [14]:

$$\rho \cdot c(T) \cdot \frac{\partial T}{\partial t} = \frac{\partial}{\partial x}\left(k(T) + \frac{\partial T}{\partial x}\right) + \frac{\partial}{\partial y}\left(k(T) + \frac{\partial T}{\partial y}\right) + \frac{\partial}{\partial z}\left(k(T) + \frac{\partial T}{\partial z}\right) \tag{13}$$

ρ defines the material density, while $c(T)$ defines the temperature dependent specific heat capacity. $\frac{\partial T}{\partial t}$ and $k(T)$ is respectively the change of temperature with respect to time and the temperature dependent thermal conductivity, while $\frac{\partial T}{\partial (x,y,z)}$ is the temperature gradient in the respective spatial direction [14].

Conduction is incorporated in the model via the coupled thermal-mechanical solution approach.

4. LS-DYNA Model

The non-linear coupled thermal-mechanical analysis incorporates the thermal heat transfer problem together with the mechanical problem in one combined simulation. This enables the estimations of thermal introduced stresses and strains based on temperature dependent material properties. The mechanical problem is solved implicitly and the thermal problem is solved using a diagonally scaled conjugate gradient iterative solver.

The LS-DYNA model consists of the three parts: a top plate, a bottom plate and the welding seam, as illustrated by Fig. 5 and 6.

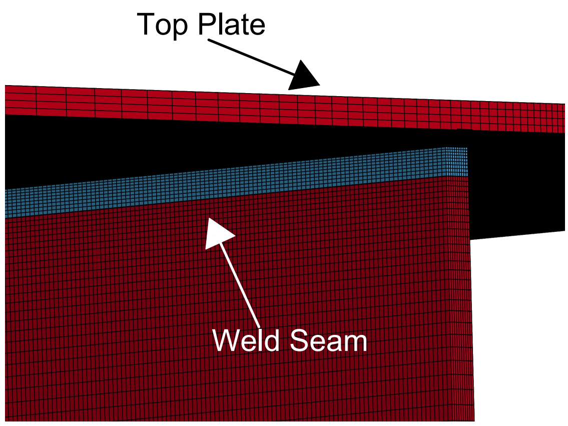

Fig. 5 Illustration of weld seam and top plate.

The dimensions of the parts are presented in Tab. I.

Tab. I Dimensions of the LS-DYNA parts.

Part	Length [mm]	Width [mm]	Thickness [mm]
Top Plate	120	100	1.5
Bottom Plate	100	48.5	1.5
Weld Seem	100	1.5	1.5

In order to replicate the fixture used in the experimental set-up, two boundary conditions, illustrated in Fig. 6, are implemented in the model.

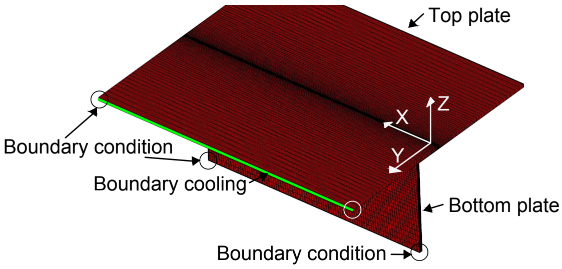

Fig. 6 LS-DYNA model containing the two defined boundary conditions.

These boundary conditions eliminate translation and rotation in any direction. Furthermore, a temperature boundary condition is implemented in the model to replicate the cooling from the experimental fixture.

4.1 Discretisation

The mesh discretisation of the model, which is performed in the software LS-INGRID, uses a linear bias mesh strategy. This strategy adjusts the element size based on the distance from the weld seam to the element, hence eliminating unnecessarily small elements far away from the weld. The mesh is constructed based on guidelines proposed by [19]:

- A minimum of two elements pr. beam radius.
- A minimum of three elements in the thickness of the welded plate.

This is done to ensure that an adequate number of elements are used to achieve the desired accuracy. It must however be noted, that it has not been possible to strictly follow the guidelines due limitations on the computational power; hence it has been chosen to use two elements pr. beam diameter.

4.2 Time-Step

According to [20], one of the major issues encountered, when simulating the LBW process, is 'time skipping'. This phenomenon occurs as a result of an error in the discretisation of the thermal time-step, and causes the heat source to skip across the blank surface. In order to overcome this issue, [20] has suggested a guideline for the thermal time-step, stated as:

- Minimum four time-steps to cover the molten zone.

Following this suggestion, the thermal time-step can be calculated based on the experimental parameters of a welding speed of $20\ \frac{mm}{s}$, a molten zone of $1.28\ mm$ and a simulation time of $5\ s$.

$$\Delta t_{thermal} = \frac{1}{4} \cdot \left(\frac{1.28\ mm}{20\ \frac{mm}{s}} \right) = 0.016\ s \tag{14}$$

The mechanical implicit time-step has been chosen based on an empirical test using different implicit time-step sizes. The time-step was evaluated based on accuracy of the solution and computational time. The implicit time-step has been set to $0.25\ s$.

4.3 Implementation of Heat source

The double-ellipsoidal volumetric heat source model is implemented in the LS-DYNA model via the DEFINE_FUNCTION keyword option. This option enables the implementation of user defined functions, which are programmed in the language C.

The heat source function is defined in a separate text file, where the power input Q, movement of the heat source and the Goldak parameters are defined and included in LS-DYNA. The output from the heat function is the calculated power density distribution, applied to the blank through the LOAD_HEAT_GENERATION keyword option.

By coding the heat source function manually, it is possible to implement a simple control algorithm for the movement of the heat source. While moving the heat source, the coordinates of all surface elements are identified. This is done to ensure, that only the elements within the ellipsoid are directly affected by the heat flux from the laser beam, in relation to the calculated Gaussian distribution. By simply ensuring that the 2D ellipsoid equation is fulfilled, this can be achieved; hence equation (15) must be true for all the considered elements.

$$\left(\frac{x^2}{c_i^2} \right) + \left(\frac{y^2}{a^2} \right) = 1 \tag{15}$$

4.4 Material Models

In order to set up a coupled thermal-mechanical analysis, all parts in the model need to be assigned temperature dependent material properties by using temperature dependent material models in LS-DYNA.

The material models used for the top and bottom plate are MAT_ELASTIC_PLASTIC_THERMAL and MAT_THERMAL_ISOTROPIC. The first of which is used to calculate the mechanical response to a temperature change via temperature dependent material coefficients including Young's moduli, Poisson's ratio, coefficient of thermal expansion, yield stress and plastic hardening moduli. The second material model is used to calculate the thermal response to a heat source via isotropic temperature dependent thermal properties, including heat capacity and thermal conductivity.

In order to replicate the fusion between the top and bottom plate, the weld seam is assigned the 270-CWM material model. This material model is a thermo-elastic-plastic model with kinematic hardening, that allows material creation as well as annealing triggered by temperature. Hence, making it possible for the material to be in a so called 'ghost' stage, where its properties are dictated by very low stiffness, no thermal expansion and no thermal conductivity. When the material is heated to the activation temperature, it changes properties and gains regular mechanical and thermal properties. The acronym CWM stands for Computational Welding Mechanics, and the model is intended to be used for simulating multi-stage weld processes [21].

5. Experimental Work

With the purpose of creating a reference database for the Goldak parameters and to provide experimental data for the model validation, a series of experimental trials are carried out. This is based on joining two 1.5 mm DS/EN 1.4301 sheet metal plates in a fusion welded T-joint by using an Nd:YAG laser beam welder. In order to perform the welding operation, the T-joint is fixed to a specially designed fixture mounted to a XY-table, moving with a constant speed of 20 mm/s.

The dimensions of the plates are presented in Tab. I, while detailed specifications of the experimental set-up are evident from Tab. II.

Tab. II The laser system and specifications [22].

Laser	IPG YLS-3000-SM
Wave length, λ	1076 nm
Beam quality, M^2	1.2
Optics	Modified HighYag BIMO
Focal length	470 mm
Collimation length	200 mm
Shielding of laser beam	Air from nozzle
XY-table	Q-SYS model 0166-01

The experimental data used for model validation is acquired by using a combination of three measuring devices:

- **Thermal Imaging Camera (TIC):** For determining the temperature directly in the weld seam after the heat source has passed. Serves primarily as a means to validate the implementation of the heat source.
- **Type K thermocouples (TC):** Recording of the temperature history at specific positions for point validation of the temperature distribution away from the weld. As the TCs are placed at a distance from the weld zone, their main purpose to indicate significant errors in the material data and the modelling of the heat dissipation.
- **Coordinate Measuring Machine (CMM):** Measuring of the welding-induced distortion of the top plate at proximity to the edge. Validation of the welding-induced distortions is performed using the CMM.

The points of data acquisition are illustrated in Fig. 7.

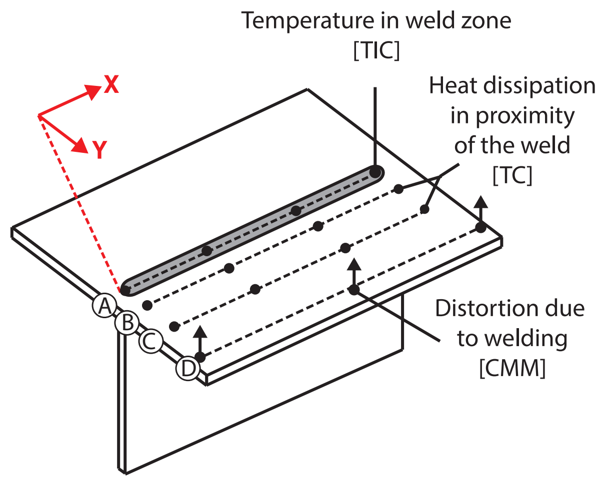

Fig. 7 Illustration of data points where A, B, C and D label each row of points, while numbers label each column.

5.1 Procedure for Validation

Three specimens have been welded at three different power inputs: $Q_{-10\%}$, Q_r and $Q_{+10\%}$, corresponding to the measured power inputs of 1.24, 1.42 and 1.62 kW. The purpose of this is to establish and possibly enhance the models ability to predict the temperature distribution and welding-induced strains at power inputs different from the reference power input Q_r, at which the model is validated in. The reference specimens, welded at a power input of Q_r, have been investigated experimentally to determine the Goldak parameters by measuring the fusion zone (FZ) via a microscopic analysis. The image used for determining the Goldak parameters is illustrated by Fig. 8.

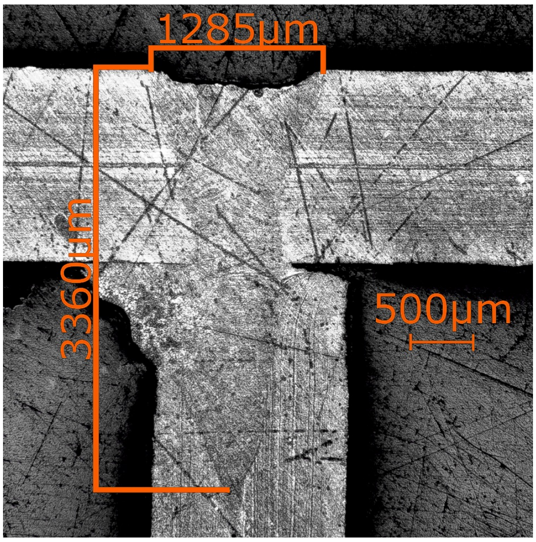

Fig. 8 Microscopic image of the weld used for determining the Goldak parameters.

Implementing the determined Goldak parameters in the LS-Dyna model, and subsequently comparing the temperatures acquired by the TICs and TCs to the corresponding data from the model, serves as a means to determine the experimental efficiency η and to validate the model. This is done through an iterative process, starting at $j = 1$ and denoting $Q^{(j)}$ as the varying power input. Hence, $Q^{(j)}$ is reduced per update until a satisfying efficiency has been obtained and the model is validated.

For evaluating the models performance at the power inputs $Q_{-10\%}$ and $Q_{+10\%}$, a two phase approach is applied. For the first phase, it is assumed, that all variables and parameters are unchanged from the reference weld, except from the power inputs $Q_{-10\%}$ and $Q_{+10\%}$. The second phase consists of analytically estimating the Goldak parameters for the power inputs $Q_{-10\%}$ and $Q_{+10\%}$. This is done by applying the approach outlined in Section 2 and by assuming a constant penetration depth, or b of the Goldak parameters, compared to those of the reference power input Q_r. The purpose of this approach is to investigate, if it is possible to increase the process window of the model by estimating the Goldak parameters.

The procedure for validation of the LBW process can described by the flow diagram in Fig. 9.

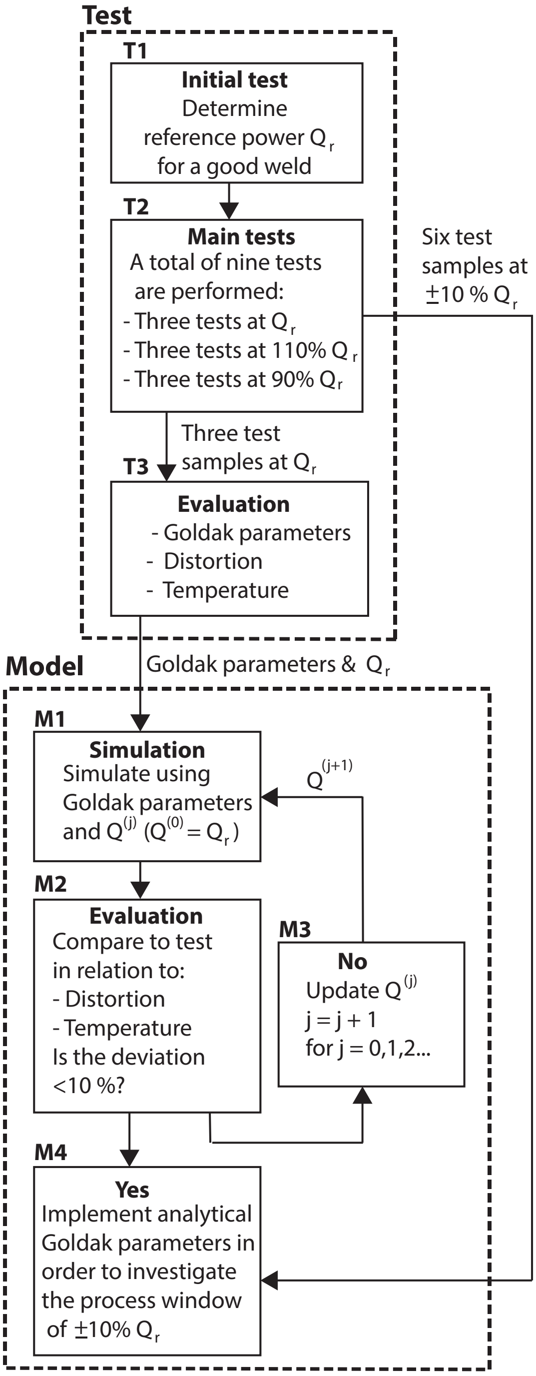

Fig. 9 Flow diagram of the validation.

6. Results and Discussion

At the determined efficiency η of 0.8 and the reference power input Q_r of 1420 W, the model has a maximum deviation of 7.53%, when comparing the temperature peaks at a series of specified points between the model and the experimental data. Comparing the temperature at the same points, but at $t = 20\ s$, having allowed the specimen to cool, yields a maximum deviation of 5.07%. As the validation criteria is set to 10%, the deviations are below the limit; hence, the model fulfils the validation criteria. A graph of the temperature in the specific points is illustrated in Fig. 10.

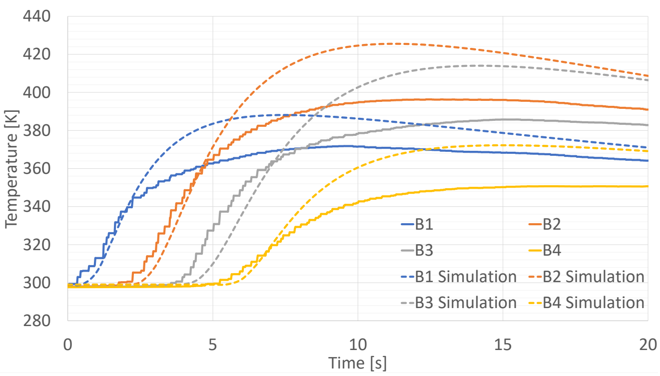

Fig. 10 Comparison of the temperature at specific between the model and experimental data.

Varying the power input by $Q_{+10\%}$ and $Q_{-10\%}$, while keeping the remaining parameters constant, showed no significant changes in the temperature deviations, evaluated at the same points as earlier. Furthermore, performing an analytical estimation of the Goldak parameters showed a nearly identical temperature distribution compared to not having changed the Goldak parameters. This can be due to the fact, that the temperatures are measured at a minimum of $8\ mm$ from the weld pool, thus it has not been possible to observe the direct changes of the heat flux distribution. This could possibly be solved by measuring the temperature directly in the weld pool.

A maximum welding induced distortion of $0.213\ mm$, occurs in the T-joint's top plate, at the edge parallel with the X-axis. It must however be noted, that it has not been possible to validate the distortion, as the variance in the measured data is too excessive to be representative. An increase in the sample size of the welded specimens, combined with measuring the distortion directly in the laser welding fixture, could decrease the variance.

7. Conclusion

Using LS-DYNA, the LBW process has been simulated by performing a non-linear coupled thermal-mechanical analysis to replicate and predict both the temperature distribution and the welding induced distortion of a T-joint. This has been done by utilizing a conduction heat transfer based model in the form of a double-ellipsoid heat flux distribution to model the heat source of the laser beam. In an effort to enhance the models predictive abilities, an analytical approach has been applied to determine the Goldak parameters for power inputs at $\pm 10\%$ of the reference Q_r.

Based on the simulation, the following conclusions can be drawn:

- It is possible to predict the temperature distribution of a laser welded component within a reasonable error margin.
- Slightly varying the power input does not yield significant changes in the temperature distribution.
- Determining the Goldak parameters through an analytical approach, while assuming a constant penetration depth, does not lead to noticeable different results, compared to maintaining the Goldak parameters.

To expand the current model, introducing a simulation for the microstructural phase changes present in the weld is a natural next step. It has been shown that a weld composition with at least 5-30% has a profound effect on reducing the presence of cracks within the weld [23]. It has also been shown that if too much ferrite is present in the weld, its corrosion resistance will be reduced [24]. If the prediction of the microstructural changes, and thus the content of ferrite present in the weld could be performed, it would be advantageous for the process.

Acknowledgement

The authors of this work gratefully acknowledge Sintex for sponsoring the 5th MechMan symposium. Furthermore, a sincere thanks must be directed to our supervisor Benny Endelt, co-supervisor Morten Kristiansen, Associate Professor Erik A. Jensen and Grundfos for their guidance and collaboration.

References

[1] M. Zain-Ul-Abdein, D. Nelias, J. F. Jullien, and D. Deloison, "Experimental investigation and finite element simulation of laser beam welding induced residual stresses and distortions in thin sheets of aa 6056-t4," Materials Science and Engineering: A, vol. 527, no. 12, pp. 3025–3039, 2010.

[2] M. Zhao, "Numerical simulation of penetrated weld pool geometry and surface deformation in tig welding," Chinese Journal of Mechanical Engineering, vol. 42, no. 10, p. 203, 2006.

[3] K. Kazemi and J. A. Goldak, "Numerical simulation of laser full penetration welding,"

Computational Materials Science, vol. 44, no. 3, pp. 841–849, 2009.
[4] M. Zain-Ul-Abdein, D. Nelias, J.-F. Jullien, and D. Deloison, "Prediction of laser beam welding-induced distortions and residual stresses by numerical simulation for aeronautic application," Journal of Materials Processing Technology, vol. 209, no. 6, pp. 2907–2917, 2009.
[5] G. Moraitis and G. Labeas, "Residual stress and distortion calculation of laser beam welding for aluminum lap joints," Journal of Materials Processing Technology, vol. 198, no. 1-3, pp. 260–269, 2008.
[6] T. Kloppel, A. Erhart, A. Haufe, and T. Loose, "Recent developments in ls-dyna to close the virtual process chain for forming, press hardening and welding," Key Engineering Materials, vol. 651-653, pp. 1312–1318, 2015.
[7] S. Bag, D. V. Kiran, A. A. Syed, and A. De, "Efficient estimation of volumetric heat source in fusion welding process simulation," Welding in the World, vol. 56, no. 11-12, pp. 88–97, 2012.
[8] D. Gery, H. Long, and P. Maropoulos, "Effects of welding speed, energy input and heat source distribution on temperature variations in butt joint welding," Journal of Materials Processing Technology, vol. 167, no. 2-3, pp. 393–401, 2005.
[9] D. Rosenthal, "The theory of moving sources of heat and its application to metal treatments," Trans. Am. Soc. mech. Engrs, vol. 43, no. 11, pp. 849–866, 1946.
[10] V. Pavelic, R. Tanbakuchi, U. O.A., and Myers., "Experimental and computed temperature histories in gas tungsten arc welding of thin plates," Welding Journal Research Supplement, vol. 48, pp. 295–301, 1969.
[11] J. Goldak, A. Chakravarti, and M. Bibby, "A new finite element model for welding heat sources," Metallurgical Transactions B, vol. 15, no. 2, pp. 299–305, 1984.
[12] M. J. Bibby, J. A. Goldak, and G. Y. Shing, "A model for predicting the fusion and heat affected zone sizes of deep penetration welds," Canadian Metallurgical Quarterly, vol. 24, no. 1, pp. 101–105, 1985.
[13] N. Christensen, V. Davies, and K. Gjermundsen, "The distribution of temperature in arc welding," British Welding Journal, vol. 12, no. 2, pp. 54–75, 1965.
[14] Y. A. Cengel and A. J. Ghajar, Heat and Mass Transfer: Fundamentals and Applications EES DVD for Heat and Mass Transfer, 4th ed. McGraw-Hill, 2010, no. ISBN:0077366646.
[15] "Convection heat transfer coefficients table chart," http://www.engineersedge.com/heat_transfer/convective_heat_transfer_coefficients__13378.htm, accessed: 2017-05-06.
[16] R. Siegel and J. R. Howell, Thermal Radiation Heat Transfer, 4th ed. Taylor and Francis, 2001, no. ISBN:1560328398.
[17] A. Shapiro and D. Lo, "Heat transfer and coupled thermal stress problems with ls-dyna," DYNAMORE, 2009.
[18] "Table of emissivity of various surfaces," http://www.czlazio.com/tecnica/Tabella%20delle%20Emissivit%C3%A0.pdf, accessed: 2017-05-06.
[19] L. Zhang, E. Reutzel, and P. Michaleris, "Finite element modeling discretization requirements for the laser forming process," International Journal of Mechanical Sciences, vol. 46, no. 4, pp. 623–637, 2004.
[20] T. Loosea, M. Bernreutherb, B. Grosse-Wohrmannb, J. Hertzerb, and U. Gohner, "Shape project ingenieurburo tobias loose: Hpcwelding: Parallelized welding analysis with ls-dyna," Partnership for Advanced Computing in Europe, pp. 1–14, 2016.
[21] L. S. T. C. (LSTC), MATERIAL USER'S MANUAL, VOLUME 2. Livermore Software Technology Corporation, 2016.
[22] M. Kristiansen, J. Selchau, F. O. Olsen, and K. S. Hansen, "Quality and performance of laser cutting with a high power sm fiber laser," Proceedings of The 14th Nordic Laser Materials Processing Conference NOLAMP 14, vol. 14, no. ISBN:978-91-7439-689-8, pp. 109–120, 2013.
[23] F. C. Hull, "Effect of delta ferrite on hot cracking of stainless steel," Welding Journal, pp. 399–409, 1967.
[24] J. C. Lippold and D. J. Kotecki, Welding metallurgy and weldability of stainless steels, 1st ed. Wiley, 2005, no. ISBN:0-471-47379-0-5.